Theoretical study of stereodynamics for the $O(^3P) + H_2 \rightarrow OH + H$ reaction*

Liu Shi-Li(刘世莉) and Shi Ying(石 英)†

Institute of Atomic and Molecular Physics, Jilin University, Changchun 130012, *China*

(Received 1 June 2010; revised manuscript received 28 July 2010)

This paper employs the quasi-classical trajectory calculations to study the influence of collision energy on the title reaction on the potential energy surface of the ground $^3A'$ triplet state developed by Rogers *et al.* (*J. Phys. Chem.* A 2000 **104** 2308). It calculates the product angular distribution of $P(\theta_{\rm r})$, $P(\phi_{\rm r})$ and $P(\theta_r, \phi_{\rm r})$ which reflects vector correlation. The distribution $P(\theta_{\rm r})$ shows that product rotational angular momentum vectors $\boldsymbol{j}'$ of the products are strongly aligned along the relative velocity direction $\boldsymbol{k}$. The distribution of $P(\phi_{\rm r})$ implies a preference for left-handed product rotation in planes parallel to the scattering plane. Four different polarisation-dependent cross-sections are also presented in the centre-of-mass frame. Results indicate that OH is sensitively affected by collision energies of H_2.

Keywords: quasi-classical trajectory, polarisation-dependent generalised differential cross-sections, stereodynamics

PACS: 34.50.Lf, 82.20.Kh **DOI:** 10.1088/1674-1056/20/1/013404

1. Introduction

The dynamics of the reaction $O(^3P)+H_2$ are known to be a major participant in combustion[1] and are also important in upper atmosphere reactions[2,3] and interstellar chemistry.[4,5] As a typical atom-molecule reaction, it is the prototype system for testing the quality of new theories and experiments. Its fundamental importance has led to reports on numerous experimental studies[6−13] and potential energy surface (PES) and dynamic calculations[14−21] over the last three decades. Specifically, Garton *et al.*[7] obtained the relative excitation function from a crossed molecular beams apparatus, and the results were in good agreement with the quantum wave packet calculation. Robie *et al.*[8,9] measured the ratio of intramolecular kinetic isotope effect using the laser-induced fluorescence (LIF) method and found very strong negative temperature dependence. Han *et al.*[11] studied the title reaction by LIF detection of the OH product and observed the non-statistical rotational state population of $X^2\Pi$. Rogers *et al.*[14] theoretically constructed a PES based on extensive high quality ab initio calculations. Maiti and Schatz[15] employed the quasi-classical trajectory (QCT) surface hopping method to investigate the nonadiabatic dynamics of $O(^3P)+H_2$. Chu *et al.*[17,18] presented the quantum study of spin-orbit-induced intersystem crossing effects in the $O(^3P)+H_2$ reaction and demonstrated that the spin-orbit coupling among the triplet states of different symmetries greatly contributes to intersystem crossing. Balakrishnan,[19] Sultanov and Balakrishnan,[20] and Braunstein *et al.*[21] recently reported their adiabatic dynamics calculations on the $O(^3P) + H_2 \rightarrow OH + H$ reaction, finding consistent results between these calculated total reaction cross-sections and experiments. Owing to experimental and theoretical breakthroughs, there is a renewed interest in the title reaction. Recently, a more robust variation of the method has been improved,[22] called the moving boundary truncation (MBT) method, it can significantly reduce the number of grid points needed to perform accurate wave packet propagation while maintaining stability. Significant improvements have been made which allow the MBT method to be applied to any PES and used with any propagation method.

Previous studies have basically dealt with scalar properties. To reveal the dynamics of the title reaction fully, studying not only the scalar properties but also the vector properties is important. The vector correlation between the reagent and product can provide valuable information about the stereodynamics of the chemical reaction. In 2009, Wei *et al.*[23] presented the result that vector properties are sensitively affected by vibrational excitation.

To shed more light on the stereodynamics of the

*Project supported by Jilin University, China (Grant No. 419080106440).

†Corresponding author. E-mail: shi_ying@jlu.edu.cn

© 2011 Chinese Physical Society and IOP Publishing Ltd

dynamics of O(^{3}P)+H_2(0,0) reaction, we use the QCT method to study the product rotational polarisation for the title dynamics on the singlet lowest $^3A'$ PESs and the influence of collision energies on the vector correlations of the product.

2. Theory

2.1. The QCT calculations

The calculation method of the QCT has been described in Refs. [24]–[26]. The classical Hamilton's equations are numerically integrated for motion in three dimensions. In our calculation, rotational levels of the reactant molecules are taken as $v = 0$ and $j = 0$, respectively. Batches of 50000 trajectories are run for collision energies chosen as 15, 30, and 45 kcal/mol. The integration step size is 0.1 fs. Accuracy of the numerical integration is verified by checking the conservation of the total energy and total angular momentum for each trajectory.

2.2. Rotational alignment parameter

The degree of polarisation of angular momentum $\boldsymbol{j}'$ of the product molecule can be visualised through the centre of mass (CM) orientation and alignment parameters in Fig. 1.

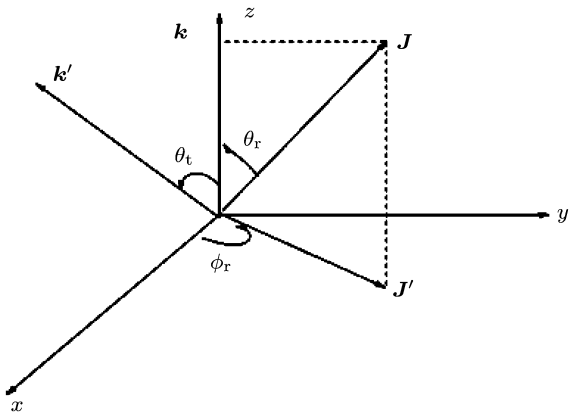


Fig. 1. The CM coordinate system used to describe $\boldsymbol{k}$, $\boldsymbol{k}'$, and $\boldsymbol{j}'$ distributions of the reaction O(^{3}P)+H_2(0,0).

The distribution function of the angular momentum $\boldsymbol{j}'$ of the product molecule can be expanded in a set of Legendre polynomials, which describes the correlation between $\boldsymbol{j}'$ and the relative velocity vector $\boldsymbol{k}$.[27,28]

$$f(\theta_{\rm r}) = \sum_l a_l p_l(\cos\theta_{\rm r}), \tag{1}$$

where $l = 2$ indicates the product rotational alignment,

$$\langle P_2(j'.z)\rangle = \frac{1}{2}[3\cos^2\theta - 1]. \tag{2}$$

2.3. Polarisation-dependent different cross-sections (PDDCSs)

The full angular distribution of the triple vector correlations $\boldsymbol{k}$, $\boldsymbol{k}'$, and $\boldsymbol{j}'$ of the product molecule can be represented by a set of PDDCSs in the CM coordinate. In this chosen coordinate, the z-axis is parallel to the reagent relative velocity $\boldsymbol{k}$, and the y-axis is perpendicular to the xz plane containing $\boldsymbol{k}$ and $\boldsymbol{k}'$. To describe the vector correlation of the reaction of the atom-diatomic molecule fully, the correlated centre-of-mass function is written as[29,30]

$$P(\cos\theta, \cos\theta_{\rm r}, \phi_{\rm r}) = \frac{1}{4\pi}\sum_{k=0}^{\infty}\sum_{q=-k}^{k}(2k+1) \times \frac{2\pi}{\sigma}\frac{{\rm d}\sigma_{kq}}{{\rm d}\omega}c_{kq}(\theta_{\rm r}, \phi_{\rm r})^*, \tag{3}$$

where $(1/\sigma)({\rm d}\sigma_{kq}/{\rm d}\omega_{\rm t})$ describes the generalised PDDCSs. The functional form can be referred to in the Refs. [31]–[33]. In our investigation, we only compute for $(2\pi/\sigma)({\rm d}\sigma_{00}/{\rm d}\sigma_{\omega_t})$, $(2\pi/\sigma)({\rm d}\sigma_{20}/{\rm d}\sigma_{\omega_t})$, $(2\pi/\sigma)({\rm d}\sigma_{22^+}/{\rm d}\sigma_{\omega_t})$ and $(2\pi/\sigma)({\rm d}\sigma_{21^-}/{\rm d}\sigma_{\omega_t})$. The four PDDCSs are expanded up to $\boldsymbol{k} = 7$.

The usual distribution function $P(\theta_{\rm r})$ describing the two vector $\boldsymbol{k}-\boldsymbol{j}'$ correlation is expanded in a series of Legendre polynomials [34]–[36]. In this research, the distribution $P(\theta_{\rm r})$ is expanded up to $\boldsymbol{k} = 18$ for good convergence.

$$P(\theta_{\rm r}) = 1/2\sum_k [k]a_0^k p_k(\cos\theta_{\rm r}). \tag{4}$$

The dihedral anglular distributions of the $\boldsymbol{k}-\boldsymbol{k}'-\boldsymbol{j}'$, $\boldsymbol{k}-\boldsymbol{k}'-\boldsymbol{l}$ ($\boldsymbol{l}$ is the reagent orbital angular momentum) and $\boldsymbol{k}-\boldsymbol{k}'-\boldsymbol{l}'$ ($\boldsymbol{l}'$ is the product orbital angular momentum) in the three-vector correlation are characterised by the angles $\phi_{\rm r}$, $\boldsymbol{l}$, and $\boldsymbol{l}'$, respectively. The distribution of the dihedral angle $\phi_{\rm r}$ can be expanded as a Fourier series:[35–37]

$$P(\phi_{\rm r}) = 1/2\pi\Big(1 + \sum_{n_{\rm even}\geq 2} a_n\cos(n\phi_{\rm r}) + \sum_{n_{\rm odd}\geq 1} b_n\sin(n\phi_{\rm r})\Big). \tag{5}$$

In this work, $P(\phi_{\rm r})$ is expanded up to $n = 24$.

Thus, the spatial distribution of product rotational angular momentum can be launched as[38]

$$P(\theta_{\rm r},\phi_{\rm r}) = \frac{1}{4\pi}\sum_{kq}[k]a_q^k c_{kq}(\theta_{\rm r},\phi_{\rm r})^* = \frac{1}{4\pi}\sum_{k}\sum_{q\geq 0}[a_{a\pm}^k\cos(q\phi_{\rm r}) - a_{q\mp}^k\,{\rm i}\sin(q\phi_{\rm r})]c_{kq}(\theta_{\rm r},0), \quad (6)$$

where a_n and b_n are given by $a_n = 2\langle\cos(n\phi_{\rm r})\rangle$ and $b_n = 2\langle\sin(n\phi_{\rm r})\rangle$.

In our calculation, $P(\theta_{\rm r},\phi_{\rm r})$ is calculated with $\boldsymbol{k} = 7$ to obtain good convergence.

2.4. The PES

In the computation, the $H_2O(^3A')$ generalized London-Eyring-Polariyi-Sato (GDLP) PES of Rogers *et al.*[14] is used. The GDLP PES of the title reaction in the $^3A'$ state is the best fit to the *ab initio* data calculated by Rogers at collinear abstraction geometry. The GDLP PES is also characterised by an abstraction saddle-point position at $R_{\rm HH} = 2.3096a_0$ and $R_{\rm OH} = 1.7050a_0$. The reaction barrier is 13.22 kcal/mol (1 cal=4.1868 J) above the $O(^3P)+H_2$ asymptote limit. We choose three energies beyond the energy of the barrier to study the influence of collision energy on the title reaction on the PES.

3. Results and discussions

The calculated results of distribution $P(\theta_{\rm r})$ for the three collision energies ($E_{\rm T}$ = 15, 30 and 45 kcal/mol) of the $O(^3P)+H_2(0,0)$ reaction are depicted in Fig. 2. The distributions $P(\theta_{\rm r})$ representing the $\boldsymbol{k}-\boldsymbol{j}'$correlation lead to the conclusion that product rotational alignment is very strong. For the three collision energies, Fig. 2 clearly illustrates that the peak of $P(\theta_{\rm r})$ is at $\theta_{\rm r} = 90°$ and is symmetric with respect to 90° because of the planar symmetry of the system. This implies that the product rotational angular momentum vector is strongly aligned along the direction perpendicular to the relative velocity direction. The peak of $P(\theta_{\rm r})$ is not sensitive to the collision energy. However, as seen in Fig. 2, the product rotational alignment effect is strongest at the collision energy of 30 kcal/mol.

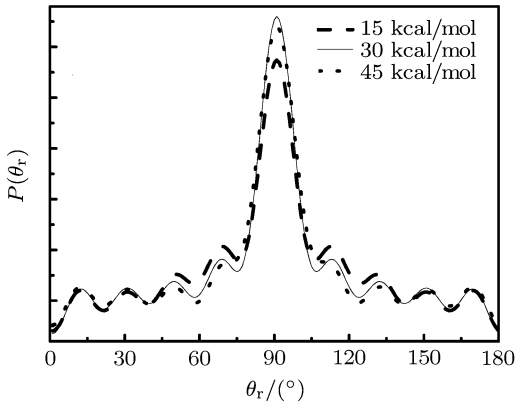


Fig. 2. Distribution $P(\theta_{\rm r})$ reflecting the $\boldsymbol{k}-\boldsymbol{j}'$ correlation at three collision energies.

To understand the correlation of $\boldsymbol{k}-\boldsymbol{k}'-\boldsymbol{j}'$, we calculate the dihedral angle distribution $P(\phi_{\rm r})$, the results are shown in Fig. 3. The $P(\phi_{\rm r})$ tends to be antisymmetric with respect to the scattering plane, directly reflecting the strong polarisation of the angular momentum induced by the PES. For the three collision energies, the $P(\phi_{\rm r})$ distribution has only one peak of every curve appearing at 270°. This demonstrates that the rotational angular momentum vector of the product OH is oriented along the negative direction of y-axis of the CM frame.

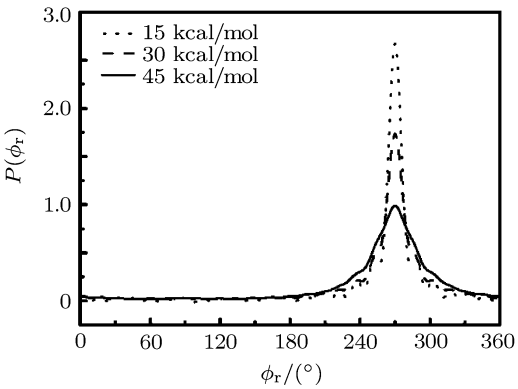


Fig. 3. Distribution $P(\phi_{\rm r})$describing the dihedral angle distribution of $\boldsymbol{j}'$ with respect to the $\boldsymbol{k}-\boldsymbol{k}'$ plane at three collision energies.

The distribution $P(\phi_{\rm r})$ is antisymmetric and is strongly affected by the collision energies. Antisymmetry most likely results from the repulse energy between H–H atoms, leading to the violation of the symmetry when the reaction occurs. According to previous studies,[39−41] the distribution of the product rotational angular momentum vector is $\boldsymbol{j}' = L\sin^2\beta + j\cos^2\beta + J_1 m_{\rm A}/m_{\rm B}$, where L is the reagent orbital angular momentum, $J_1 = (\mu_{\rm BC}R)^{1/2}(r_{\rm AB}\cdot r_{\rm CB})$, $\mu_{\rm BC}$ is the reduced mass of

the BC molecule, and R is the repulsive energy. In the reaction $O(^3P) + H_2 \rightarrow OH + H$, the term $L\sin^2\beta + j\cos^2\beta$ is symmetric, whereas the term $J_1 m_A/m_B$ shows a preferential direction for the effect of repulsive energy, leading to the left-handed product rotation in planes parallel to the scattering plane. The distribution $P(\phi_r)$ strongly affected by the collisions can be attributed to two reasons. One reason is that the O atom has relatively strong absorbability to charges. At higher collision energies, the O atom rapidly and easily grips the H atom away from the HO molecule. The other reason is that the overwhelming amount of collision energy transfers into the translational energy of the product, and the contribution to the product rotational angular momentum is little. Therefore, the trend of product molecular rotational angular momentum becomes weakly aligned and oriented along the y-axis for the increasing collision energy[42]

To obtain more information about product molecule axis polarisation, the $P(\theta_r, \phi_r)$ distribution averaged over all the scattering angles is plotted in Fig. 4. In Fig. 4, the distributions $P(\theta_r, \phi_r)$ with peaks at $(90°, 270°)$ are in accordance with the distributions $P(\theta_r)$ and $P(\phi_r)$ of the OH products for the three collision energies, although there are shape differences. The graph of the distribution $P(\theta_r, \phi_r)$ indicates that the OH products are preferentially polarised perpendicular to the scattering plane, and the reaction is dominated by in-plane mechanisms.[39] The higher the collision energy is, the stronger the product rotational alignment is. The distribution $P(\theta_r, \phi_r)$ indicates that the products are strongly polarised perpendicular to the scattering plane, and the products of reaction are mainly rotating in planes parallel to the scattering plane.[43−45]

Generalised PDDCSs are used to explain the $\boldsymbol{k} - \boldsymbol{k}' - \boldsymbol{j}'$ correlation and the scattering direction of the products. The four PDDCSs of products $(2\pi/\sigma)(d\sigma_{00}/d\sigma_{\omega_t})$, $(2\pi/\sigma)(d\sigma_{20}/d\sigma_{\omega_t})$, $(2\pi/\sigma)(d\sigma_{22^+}/d\sigma_{\omega_t})$ and $(2\pi/\sigma)(d\sigma_{21^-}/d\sigma_{\omega_t})$ are drawn in Fig. 5. The PDDCS $(2\pi/\sigma)(d\sigma_{00}/d\sigma_{\omega_t})$ only describes the $\boldsymbol{k} - \boldsymbol{k}'$ correlation or the scattering direction of the product and is not associated with the orientation and alignment of the product rotational angular momentum vector $\boldsymbol{j}'$. In Fig. 5(a) the product is mainly scattered backward for the collision energies of 15 kcal/mol. With the increase in collision energy, the product becomes strongly scattered forward and weaker backward at the collision energies of 30 and 45 kcal/mol, respectively. This affirms that the scattering direction of the product OH is related to the collision energies. The PDDCS $(2\pi/\sigma)(d\sigma_{20}/d\sigma_{\omega_t})$ is the expected value of the second Legendre moment $\langle p_2(\boldsymbol{j}' \cdot z)\rangle$ shown in Fig. 5(b). The behaviour of $(2\pi/\sigma)(d\sigma_{20}/d\sigma_{\omega_t})$ shows a trend opposite to that of $(2\pi/\sigma)(d\sigma_{00}/d\sigma_{\omega_t})$, which means that $\boldsymbol{j}'$ is strongly aligned perpendicular to $\boldsymbol{k}$ at $\theta_r = 0°$ and $\theta_r = 180°$ for the three collision energies.

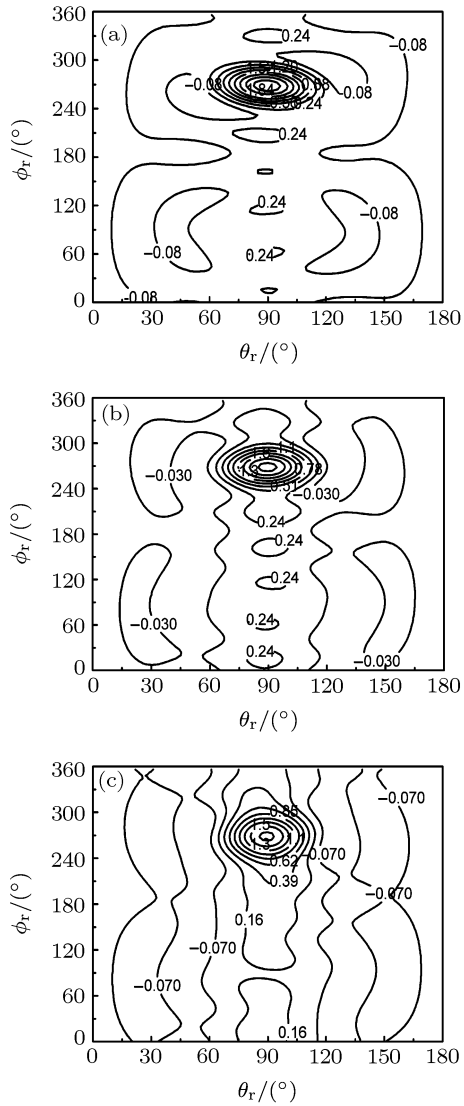


Fig. 4. Polar plots of the $P(\theta_r, \phi_r)$ distribution for three collision energies averaged over all the scattering angles (a) $E_T = 15$ kcal/mol, (b) $E_T = 30$ kcal/mol, (c) $E_T = 45$ kcal/mol.

To obtain more information from the PDDCSs and to reveal the effect of different collision energies, distributions of $(2\pi/\sigma)(d\sigma_{22^+}/d\sigma_{\omega_t})$ and $(2\pi/\sigma)(d\sigma_{21^-}/d\sigma_{\omega_t})$ are plotted in Figs. 5(c) and 5(d). Considering that PDDCSs with $q \neq 0$, we find that all PDDCSs are equal to zero at the ex-

tremities of forward and backward scattering. The value of $(2\pi/\sigma)(\mathrm{d}\sigma_{22^+}/\mathrm{d}\sigma_{\omega_t})$ at the scattering angles away from the extremities of the forward and backward directions provides information on the ϕ_r dihedral angle distribution and is non-zero at the scattering angles away from $\phi_\mathrm{r} = 0°$ and 180°. This indicates that $(2\pi/\sigma)(\mathrm{d}\sigma_{22^+}/\mathrm{d}\sigma_{\omega_t})$ is not isotropic for sideways and forward scattering products. The value of $(2\pi/\sigma)(\mathrm{d}\sigma_{22^+}/\mathrm{d}\sigma_{\omega_t})$ is negative for all scattering angles, suggesting the remarkable preference of product alignment along the y-axis. The reaction presents a consistent polarisation trend with little discordance. As seen in Figs. 5(c) and 5(d), the collision energy has considerable influence on angular distribution. The strongest polarisation of the product of the three collision energies is at about 143°, 95°, and 67°, respectively. With the decrease in collision energy, $(2\pi/\sigma)(\mathrm{d}\sigma_{22^+}/\mathrm{d}\sigma_{\omega_t})$ displays more apparent anisotropy. In Fig. 5(d), when the scattering angle is lower than 60°, the value of $(2\pi/\sigma)(\mathrm{d}\sigma_{21^-}/\mathrm{d}\sigma_{\omega_t})$ is closer to zero for the three collision energies. The PDDCS $(2\pi/\sigma)(\mathrm{d}\sigma_{21^-}/\mathrm{d}\sigma_{\omega_t})$ shows obvious isotropic characteristics when $\phi_\mathrm{r} \leq \pi/3$. The product shows stronger polarisation at the collision energy of 45 kcal/mol.

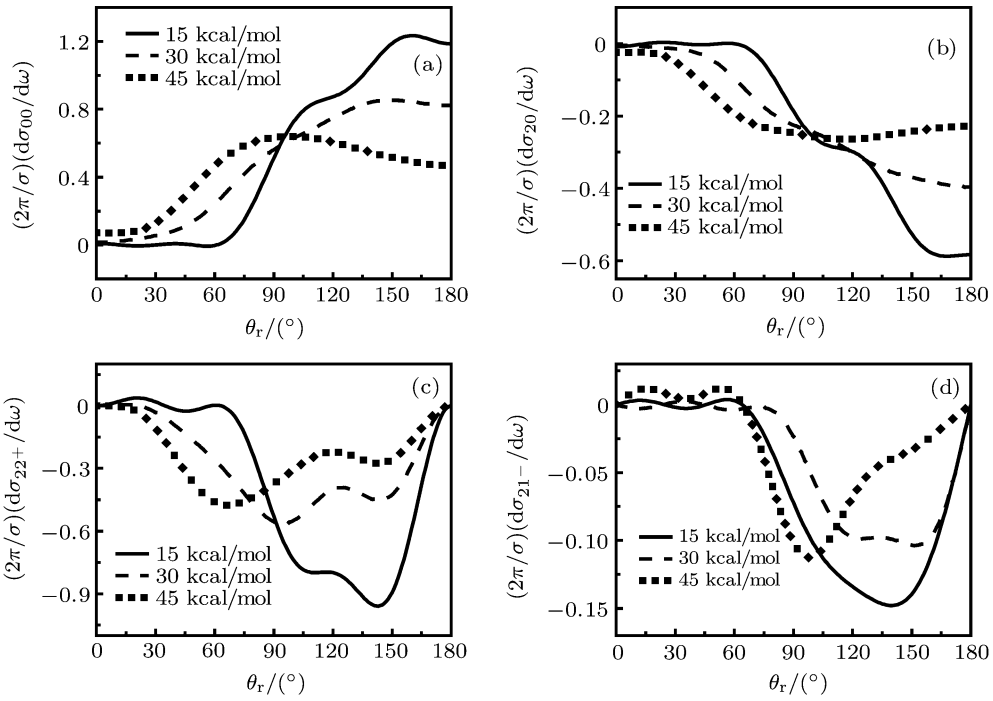


Fig. 5. The four PDDCSs of the title reaction. Solid, dashed, and short lines correspond to the reaction of collision energies 15, 30, and 45 kcal/mol, respectively.

4. Conclusions

In this paper, we studied the vector correlations between the product and reagent for the reaction $O(^3P)+H_2(0,0)$ on GDLP PES by employing a QCT method at the collision energies of 15, 30, and 45 kcal/mol. The distribution $P(\phi_\mathrm{r})$ of angles among $\boldsymbol{k} - \boldsymbol{k}' - \boldsymbol{j}'$, distribution $P(\theta_\mathrm{r})$ of the dihedral angle between $\boldsymbol{k}$ and $\boldsymbol{j}'$, and the four generalised PDDCSs was calculated. Results show that the rotational polarisation of the product presents different characteristics for different collision energies. The distribution of $P(\theta_\mathrm{r})$ suggests that the product rotational angular momentum vectors $\boldsymbol{j}'$ of the products for the title reactions are strongly aligned perpendicular to the relative velocity direction $\boldsymbol{k}$. The product rotational alignment effect is strongest at the collision energy of 30 kcal/mol. The distribution $P(\phi_\mathrm{r})$ shows that the product rotational angular momentum vector $\boldsymbol{j}'$ is oriented along the negative direction of y-axis of the CM frame and implies a preference for left-handed product rotation in planes parallel to the scattering plane when the reaction occurs. The four PDDCSs characterising the product OH predict that $\boldsymbol{j}'$ is polarised

perpendicular to $\boldsymbol{k}$ and is sensitively affected by the collision energy. With the increase in the collision energy, the product gradually scatters from backward to forward.

References

[1] Glassman 1987 *Combustion* (New York: Academic) p56
[2] Balakrishnan N 2004 *Geophys. Res. Lett.* **31** L04106
[3] Reynard L M and Donaldson D J 2001 *Geophys. Res. Lett.* **28** 2157
[4] Marcus R A 2004 *J. Chem. Phys.* **121** 8201
[5] Graff M M and Dalgarno A 1987 *Astrophys. J.* **317** 432
[6] Presser N and Gordon R J 1985 *J. Chem. Phys.* **82** 1291
[7] Garton D J, Minton T K, Maiti B, Troya D and Schatz G C 2003 *J. Chem. Phys* **118** 1585
[8] Robie D C, Arepalli S, Presser N, Kitsopoulos T and Gordon R J 1987 *Chem. Phys. Lett.* **134** 579
[9] Robie D C, Arepalli S, Presser N, Kitsopoulos T and Gordon R J 1990 *J. Chem. Phys.* **92** 7382
[10] Marshall P and Fontijn A 1987 *J. Chem. Phys.* **87** 6988
[11] Han J D, Chen X R and Weiner Brad R 2000 *Chem. Phys. Lett.* **332** 243
[12] Yang H X, Shin K S and Gardiner W 1993 *Chem. Phys. Lett.* **207** 69
[13] Dixon-Lewis G and Williams D J 1977 *Compr. Chem. Kinet.* **17** 1
[14] Rogers S, Wang D S, Kuppermann A and Walch S 2000 *J. Phys. Chem.* A **104** 2308
[15] Maiti B and Schatz G C 2003 *J. Chem. Phys.* **119** 12360
[16] Clary D C and Connor J N L 1980 *Mol. Phys.* **41** 689
[17] Chu T S, Zhang X and Han K L 2005 *J. Chem. Phys.* **122** 214301
[18] Chu T S, Zhang Y and Han K L 2006 *Int. Rev. Phys. Chem.* **25** 201
[19] Balakrishnan N 2003 *J. Chem. Phys.* **119** 195
[20] Sultanov R A and Balakrishnan N 2004 *J. Chem. Phys.* **121** 11038
[21] Braunstein M, Adler-Golden S, Maiti B and Schatz G C 2004 *J. Chem. Phys.* **120** 4316
[22] Pettey L R and Wyatt R E 2008 *J. Phys. Chem.* A **112** 13335
[23] Wei Q, Li X and Li T 2010 *Chem. Phys.* **368** 58
[24] Truhlar D G and Muckerman J T In: Bernstein R B (eds.) 1979 *A Guide for the Experimentalist* (New York: Plenum Press) p505
[25] Murrell J N, Caner S, Farantos S C, Huxley P and Varandas A J C 1984 *Molecular Potential Energy Functions* (New York: Wiley) p29
[26] Han K L, He G Z and Lou N Q 1996 *J. Chem. Phys.* **105** 8699
[27] Prisant M G, Rettner C T and Zare R N 1981 *J. Chem. Phys.* **75** 2222
[28] Liu Y F, Meng H Y and Han K L 2005 *Chem. Phys.* **309** 223
[29] Shafer-Ray N E, Orr-Ewing A J and Zare R N 1995 *J. Phys. Chem.* **99** 7591
[30] Chen M D, Han K L and Lou N Q 2003 *J. Chem. Phys.* **118** 4463
[31] Liu Y F, Gao Y L, Shi D H and Sun J F 2009 *Chem. Phys.* **364** 46
[32] Xu W W, Liu X G and Zhang Q G 2008 *Mol. Phys.* **106** 1787
[33] Li W L, Wang M S, Yang C L, Liu W W, Sun C and Ren T Q 2007 *Chem. Phys.* **337** 93
[34] Brouard M, Lambert H M, Rayner S P and Simons J P 1996 *Mol. Phys.* **89** 403
[35] Zhang W Q, Cong S L, Zhang C H, Xu X S and Chen M D 2009 *J. Phys. Chem.* A **113** 4192
[36] Wei Q, Li X and Li T 2009 *Chin. J. Chem. Phys.* **22** 523
[37] Xu W W, Liu X G, Luan S X, Sun S S and Zhang Q G 2009 *Chin. Phys.* B **18** 339
[38] Zhang W Q, Li Y Z, Xu X S and Chen M D 2010 *Chem. Phys.* **367** 115
[39] Chen M D, Han K L and Lou N Q 2002 *Chem. Phys. Lett.* **357** 483
[40] Kong H, Liu X G, Xu W W and Zhang Q G 2009 *Chin. Phys. Lett.* **26** 053102
[41] Duan L H, Zhang W Q, Xu X S, Cong S L and Chen M D 2009 *Mol. Phys.* **107** 2579
[42] Zhao J, Xu Y, Zhao X and Meng Q T 2010 *Sci. China Chem.* **53** 927
[43] Zhao J, Xu Y and Meng Q T 2009 *Can. J. Phys.* **87** 1247
[44] Zhao J, Xu Y and Meng Q T 2009 *J. Phys.* B: *At. Mol. Opt. Phys.* **42** 165006
[45] Zhang C H, Zhang W Q and Chen M D 2009 *JTCC* **8** 403